Decoupling between SARS-CoV-2 transmissibility and population mobility associated with increasing immunity from vaccination and infection in South America

Marcelo Fiori*† Gonzalo Bello‡ Nicolás Wschebor§ Federico Lecumberry¶
Andrés Ferragut‖ Ernesto Mordecki**

Abstract

All South American countries from the Southern cone (Argentina, Brazil, Chile, Paraguay and Uruguay) experienced severe COVID-19 epidemic waves during early 2021 driven by the expansion of variants Gamma and Lambda, however, there was an improvement in different epidemic indicators since June 2021. To investigate the impact of national vaccination programs and natural infection on viral transmission in those South American countries, we analyzed the coupling between population mobility and the viral effective reproduction number R_t. Our analyses reveal that population mobility was highly correlated with viral R_t from January to May 2021 in all countries analyzed; but a clear decoupling occurred since May-June 2021, when the rate of viral spread started to be lower than expected from the levels of social interactions. These findings support that populations from the South American Southern cone probably achieved the conditional herd immunity threshold to contain the spread of regional SARS-CoV-2 variants circulating at that time.

1 Introduction

Countries from the South America Southern cone experienced large COVID-19 epidemic waves during the first months of 2021 driven by the lack of stringent mitigation measures along with the emergence and regional spread of the Variant of Concern (VOC) Gamma and the Variant of Interest (VOI) Lambda [1]. The VOC Gamma was the predominant viral variant in Brazil, Paraguay and Uruguay; while both Gamma and Lambda circulated at similar prevalence in Argentina and Chile [2, 3, 4, 5].

Changes in different epidemic indicators from mid-June to end of August, including declining numbers of new SARS-CoV-2 cases and deaths and viral effective reproduction number (R_t) below one, support a relative control of the COVID-19 epidemic in all five countries [1]. The drivers of such epidemic control remained unclear as SARS-CoV-2 transmission could be influenced by several factors including extent of non-pharmaceutical interventions (NPIs), level of social distancing, adherence to self-care measures, transmissibility of circulating viral variants and the proportion of susceptible host [6].

Several studies demonstrate that during the pre-vaccination phase and in a context of large community transmission of the virus, when other factors as contact tracing strategies are not effective, changes in population mobility could be predictive of changes in epidemic trends and viral R_t [7, 8, 9, 10, 11, 12, 13]. More specifically, the mobility of the population tends to be in correspondence with the amount of social

*Corresponding author: mfiori@fing.edu.uy
†Instituto de Matemática y Estadística "Rafael Laguardia", Facultad de Ingeniería, Universidad de la República, Uruguay
‡Instituto Oswaldo Cruz (FIOCRUZ), Rio de Janeiro , Brazil
§Instituto de Física, Facultad de Ingeniería, Universidad de la República, Uruguay
¶Instituto de Ingeniería Eléctrica, Facultad de Ingeniería, Universidad de la República, Uruguay
‖Facultad de Ingeniería, Universidad ORT, Uruguay
**Centro de Matemática, Facultad de Ciencias, Universidad de la República, Uruguay

interactions, which in turn influences the infection rate and the viral R_t, that is, the average number of secondary cases per infectious case in a population made up of both susceptible and non-susceptible hosts.

When the viral community transmission is high, the population mobility captures the behaviour of infected population and we thus expect to see a correlation between mobility and viral R_t. Hence, in this context, a decoupling between population mobility and viral transmissions could be used as a surrogate marker of herd immunity achieved either through high vaccination and/or natural infection rates. Data from countries with advanced vaccination like Israel and the United Kingdom support this notion as in a certain time SARS-CoV-2 incidence display sustained declines despite easing of lockdown restrictions, discontinuation of face mask use in open spaces and increase in population mobility [14, 15]

In the present article, we estimate the coupling between population mobility and the R_t of SARS-CoV-2 in the five South American countries from the Southern cone. Our analyses support that mobility data was highly correlated with the viral R_t in all South American countries analyzed between January and May, 2021; however, a clear decoupling between both was evident since May-June 2021. The mean estimated threshold of immune individuals (fully vaccinated pondered by vaccine effectiveness plus natural infected) necessary to produce such decoupling varies along the five countries from 29% to 45% and a discussion trying to understand these differences is provided.

2 Results

To analyze the potential correlation between social mobility and the spread of the SARS-CoV-2, we used mobility information provided by Google [16] to estimate a candidate of proxy for the viral R_t, denoted as $\hat{R}_t$, during a time period of high viral transmission in every country (see subsection 4.2). The resulting $\hat{R}_t$ estimator was then correlated with the observed R_t estimated from the incidence data available in the Our World in Data (OWID) data base [1]. We refer the reader to Appendix A.2.1 for a brief description on how this reproduction number is estimated. The correlation between $\hat{R}_t$ and R_t provides a measure of the value of social mobility as a predictor of viral transmissions in each country, while the ratio $\hat{R}_t/R_t$ provides a measure of the coupling between both indicators. When the predicted value of the reproductive number estimated from mobility indicators (i.e. $\hat{R}_t$), is very close to the value of the reproductive number computed from daily infections data (i.e. R_t), the coupling ratio $\hat{R}_t/R_t$ is close to one.

In all five South American countries analyzed (Argentina, Brazil, Chile, Paraguay and Uruguay) we observed that during the first months of 2021, the estimated $\hat{R}_t$ was highly correlated (ρ^2 between 0.83 y 0.94) with the observed R_t about 1-2 weeks later and the ratio $\hat{R}_t/R_t$ was close to one (0.90-1.10) during the pre-vaccination and initial vaccination phases (Figure 1). We observed a high correlation between both indicators not only during the estimation period, but also during the beginning of the vaccination roll-out. These findings confirm that population mobility was a relevant driver of viral transmissions during early 2021 in all South American countries analyzed and revealed that, under a context of high community transmission, researchers can use the observed population mobility at a given time to infer the viral transmission dynamics without the typical lag of the observed R_t.

When we extended the estimation of the $\hat{R}_t$ during the vaccination roll-out period (with the same computed initial parameters), we observed a clear increase of the ratio $\hat{R}_t/R_t$ in all South American countries analyzed since late May and early June 2021, indicating that at a certain time the rate of spread of the virus started to be lower than expected from the levels of social interactions (Figure 1). We interpret such decoupling between population mobility and viral spread as a surrogate marker of conditional herd immunity, i.e. the achieved herd immunity conditioned to the social distancing policies and the circulating viral variants in each country. In order to test our method, we conducted a similar analysis in Israel, the first country to attain conditional vaccine-induced herd immunity, and Italy, one of the most severely affected countries in Western Europe. Our findings confirm that after a period of clear coupling between population mobility and viral transmission, a decisive increase of the ratio $\hat{R}_t/R_t$ was also observed at a certain time during vaccination roll-out both in Israel and Italy (Figure A.1). The decoupling time, defined as the moment when the ratio $\hat{R}_t/R_t$ finally overcomes (i.e. the last time it crosses) the value 1.10, preceded the last peak of weekly reported cases and roughly coincides with the last day when the $R_t = 1$ in each country (Figure 1),

indicating that the decoupling time was an early indicator of epidemic control.

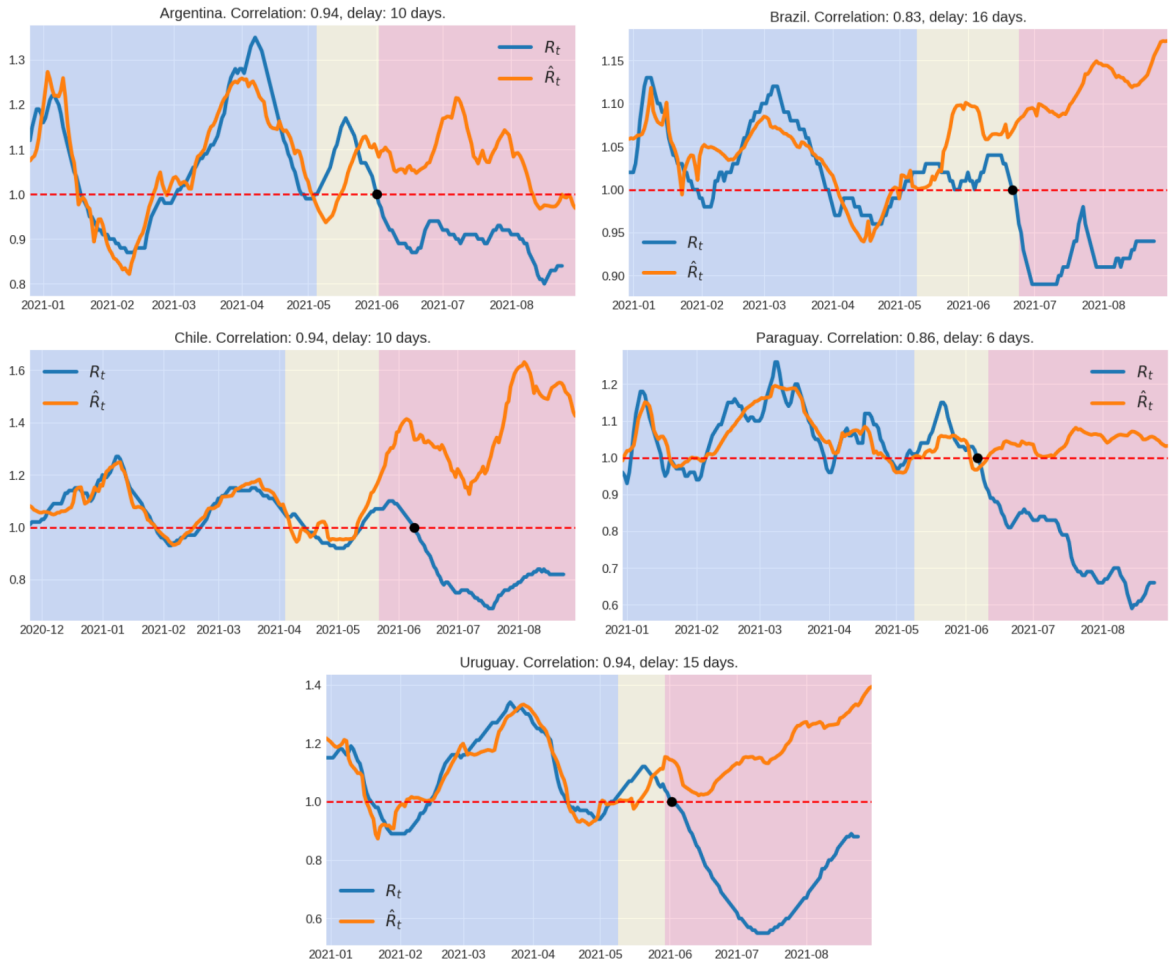

Figure 1: Temporal variation of viral effective reproduction number estimated from daily SARS-CoV-2 incidence data (R_t) and population mobility data ($\hat{R}_t$). Background colors indicate the following time periods: in blue, the time period used to fit the linear model (see Section 4.2), in yellow, the period after the fitting, but before the decoupling time, and in red after the decoupling point. The black dot corresponds to the last time the R_t was above one. The correlation corresponds to the period used to fit the model. The delay indicated is the time-shift between $\hat{R}_t$ and R_t in order to maximize their correlation in the linear regression.

The proportion of immunized population at the decoupling time could give us an idea of the conditional Herd Immunity Threshold (cHIT). In order to estimate the proportion of immune individuals around the decoupling time, we summed the estimated number of vaccine-immunized plus natural-immunized individuals. The proportion of vaccine-immunized individuals was estimated from the number of fully vaccinated individuals adjusted by the estimated vaccine effectiveness (VE) in South America [17, 18], see also [19]. The number of infected people that acquired immunity through previous infection (cumulative infection) was estimated from the cumulative number of deaths assuming a constant (age adjusted) infection fatality rate (IFR) for each country (see subsection 4.1 and Table 1). The mean estimated cHIT at the decoupling time varies along the countries from 29% in Argentina to 33% in Uruguay, 36% in Paraguay, 43% in Chile

and 45% in Brazil, although confidence intervals were very large due to uncertainties in the IFR estimates (Table 1 and Figure 2). The cHIT was reached in each country by different proportions of natural infections and vaccination (Table 1). The estimated proportion of individuals that acquired immunity through vaccination (taking into account the VE) at the decoupling time was relatively high in Chile (29%) and Uruguay (24%), but very low in Brazil (9%), Argentina (5%) and Paraguay (1%). The estimated cHIT in countries with widespread use of the inactivated vaccine Coronavac like Chile (43%) and Uruguay (33%) was similar to that estimated in Israel (42%) and Italy (31%) that only or mostly used the BNT162b2 (mRNA-based) vaccine (Figure A.2).

Country	IFR	(VIN, ADV, RNA)	T_D	% Nat-Inf	% Vac	cHIT (%)
Argentina	0.67 (0.36-1.30)	(31.1, 64.7, 04.2)	Jun. 02	26 (13-48)	06	29 (17-52)
Brazil	0.59 (0.32-1.17)	(34.4, 48.1, 17.5)	Jun. 23	40 (20-74)	11	45 (25-79)
Chile	0.73 (0.40-1.43)	(71.1, 06.9, 22.0)	May 22	20 (10-37)	40	43 (34-60)
Paraguay	0.41 (0.23-0.83)	(11.6, 26.6, 61.8)	Jun. 11	35 (18-64)	02	36 (19-64)
Uruguay	0.90 (0.49-1.56)	(59.8, 01.6, 38.6)	May 29	13 (8-24)	29	33 (27-44)
Israel	0.65 (0.35-1.27)	(0,0,100)	Feb. 28	10 (5-19)	39	42 (37-51)
Italy	1.38 (0.73-2.60)	(0,14.3,85.7)	Apr. 29	22 (11-32)	10	31 (17-38)

Table 1: IFR: infection fatality rate; VIN: percentage of virus inactivated vaccines; ADV: percentage of adenovirus vaccines; RNA: percentage of RNA vaccines [20, 21, 22, 23, 24, 25]; T_D: decoupling time; % Nat-Inf: percentage of population naturally infected at T_D; % Vac: percentage of the population fully vaccinated at T_D; cHIT (conditional herd immunity threshold): percentage of immunized population due to vaccines and natural infections at T_D. The vaccine effectiveness (VE) against SARS-CoV-2 infections was adjusted to 66% for VIN, 73% for ADV and 93% for RNA [17, 18].

3 Discussion

All countries from the South America Southern cone (Argentina, Brazil, Chile, Paraguay and Uruguay) witnessed pronounced increases in daily SARS-CoV-2 cases and deaths during the firsts months of 2021 and a clear drop in relevant epidemic metrics (cases, deaths and R_t) from mid-2021 [1]. This study demonstrates that such epidemic control was preceded by a clear decoupling of viral transmissions from population mobility, consistent with the notion that those South American countries probably attained the cHIT against SARS-CoV-2 variants Gamma and Lambda prevalent in the region, given some level of social distancing restrictions.

At the start of the pandemic, thresholds of 60-70% were given as estimates of herd immunity for SARS-CoV-2 [26]. Despite confidence intervals of estimates of percentage of immune people were very large, mostly due to uncertainties in the IFR estimates, our analyses support that the cHIT for SARS-CoV variants Gamma and Lambda in South America would be lower than 50%, ranging from 29% in Argentina to 45% in Brazil. A recent modeling study conducted in Stockholm, Sweden, also supports that this country reached the cHIT against the original and Alpha variants of SARS-CoV-2 at 23% and 33% of seroprevalence, respectively [27]. The authors conclude that cHIT for SARS-CoV-2, given limited social distancing restrictions, could be lower than initially estimated and that phenomena could be explained by population heterogeneity. By fitting epidemiological models that allow for heterogeneity in susceptibility or exposure to SARS-CoV-2 and given a basic reproduction number R_0 between 2.5 and 3, a recent study estimates that the cHIT declines from over 60% to less than 10% as the coefficient of variation increases [28]. Another study estimates that in an age-structured community with mixing rates fitted to social activity, the cHIT can be 43% if R_0 is 2.5 [29].

Our findings also support that the cHIT for SARS-CoV-2 in South America was attained through both natural and vaccinal immunity, with different relative proportions across countries. The extremely low proportion of vaccine-immune individuals in Paraguay (1%), Argentina (5%) and Brazil (9%) at decoupling

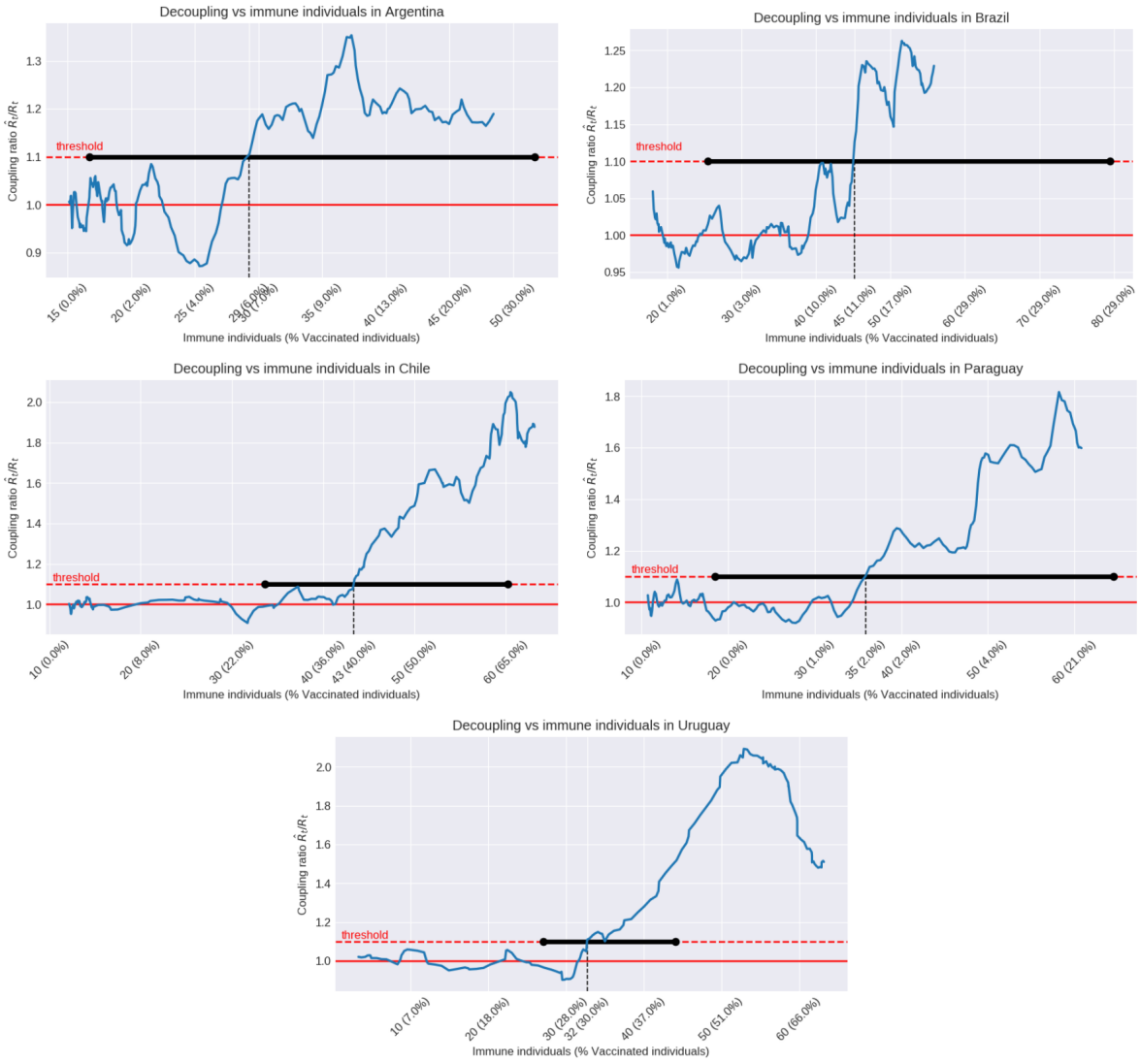

Figure 2: Coupling ratio $\hat{R}_t/R_t$ plotted with respect to the estimated percentage of immune population. During the first months of 2021 the coupling ratio varies around 1, which corresponds to the periods where the R_t and $\hat{R}_t$ are in concordance in Figure 1. Immune population includes immunity achieved by vaccination (taking into account its effectiveness) and natural infection (see subsection 4.3). The percentage of people fully vaccinated is described as well. The coupling ratio crosses the threshold (decoupling point) at percentages of immune population that varies along the five countries from 29% in Argentina to 33% in Uruguay, 37% in Paraguay, 43% in Chile and 45% in Brazil. Confidence intervals are shown in horizontal black lines. They inherit the large uncertainty in the IFR estimation (see Table 1).

time, suggest that conditional herd immunity in those countries was mostly attained by natural infections. Few studies estimated the proportion of infected individuals in South America after the large Gamma and Lambda epidemics in 2021, but some evidence from seroprevalence data support our estimations. A randomized study conducted in Paraguay between March to June 2021 gave a seroprevalence of 23.1% in Asunción and of 26.9% in the central region of the country [30] and a recent seroprevalence survey among adult individuals living in the largest Brazilian city of Sao Paulo also estimate a high proportion (45%:

39-51%) of individuals infected by SARS-CoV-2 [31].

At the other extreme, the relative proportion of vaccinal immunity at decoupling was highest in Chile (29%) and Uruguay (24%). CoronaVac accounted for most of vaccinations in Chile (75%) [32] and Uruguay (66%) [24] at decoupling time and the high incidence of SARS-CoV-2 in those countries during first months of vaccination roll-out raise concerns about the effectiveness of inactivated virus vaccines to control SARS-CoV-2 transmissions. Our results support that the widespread use of inactivated virus vaccines contributed to containing the spread of SARS-CoV-2 in Chile and Uruguay, despite abundant circulation of VOCs/VOIs and weak mitigation measures. Remarkably, the cHIT at decoupling point in Chile (43%) and Uruguay (33%) was similar to the one estimated for Israel (42%), that mostly controlled the virus expansion through vaccination with BNT162b2. These findings are consistent with recent studies of vaccine effectiveness (VE) in Chile [17], Brazil [18] and Bahrain [33] that conclude that immunization with inactivated vaccines (CoronaVac and Sinopharm) was an effective strategy at mitigating the risk for transmissions of SARS-CoV-2 VOCs, although the performance of BNT162b2 and adenovirus-based vaccines was superior.

The mean estimated cHIT varied across South American countries and several factors may explain such variability. cHIT will move upwards when more transmissible SARS-CoV-2 variants circulates in a population, but differences in the circulating SARS-CoV-2 variants do not explain variations among South American countries. Differences in the mean cHIT were observed between countries where Gamma was the most prevalent variant like Brazil (45%), Paraguay (36%) and Uruguay (33%), and also between countries where Gamma and Lambda co-circulated at high prevalence like Chile (43%) and Argentina (29%) [2, 3, 4, 5]. Differences in vaccine platforms deployed in each country might also modulate the cHIT at the decoupling time. Although we corrected the proportion of immune individuals according to the estimated VE and the proportion of each vaccine, we only considered immunity associated with fully vaccinated individuals. Previous studies, however, demonstrate some level of reduction of SARS-CoV-2 transmission after one dose of mRNA-based (46-58%), adenovirus-based (35%) and inactivated virus (16%) vaccines [17, 18, 34, 35]. Thus, we should expect that countries that used a higher proportion of mRNA-based and/or adenovirus-based vaccines like Argentina (69%) reached conditional herd immunity at apparent lower thresholds that those that mostly used inactivated virus vaccines. Moreover, it should be stressed that Argentina had a very large proportion of individuals with a single dose at the decoupling point when compared to other countries in the region where second doses were administrated in a shorter period after first dose [1]. Notably, although Brazil also used an overall high proportion of mRNA-based and/or adenovirus-based vaccines (66%), most vaccinations during first months were of inactivated vaccines [18].

Reduction of SARS-CoV-2 transmission will also depend on the vaccination strategy (who is vaccinated and when). Vaccinations programs usually begin by elderly people and go on by gradually protecting the younger population [36]. Simulation studies indicate that prioritize vaccinating of high-risk groups will minimize the number of COVID-19-related hospitalizations and deaths in the short term, but vaccination of main transmission drivers (i.e. highly mobile working age groups) would be more effective at reducing the spread of the SARS-CoV-2 [37, 38]. Given enough vaccine supplies, vaccinating the adult population uniformly at random would thus be ideal to both prevent death and severe illness in high risk groups and to curb SARS-CoV-2 transmissions in the whole population. Uruguay developed an interesting vaccination strategy that prioritized vaccination of elderly populations ($\geq$ 70 years of age) with the BNT162b2 vaccine while highly mobile working age groups were simultaneously vaccinated with CoronaVac. This more homogeneous vaccination strategy across different age groups in Uruguay might partially explain the relative low cHIT observed in this country. This may be related to the fact that, the decoupling effect due to vaccinations programs that we observe between mobility and the reproductive number is reached more abruptly than what could be expected from SIR-like models where all the population is treated homogeneously.

Our results support that proportion of immune individuals in South American populations attained a threshold enough to decoupling people mobility and viral dissemination and those countries could thus implement progressive relaxing of mitigation measures with relative safety. Such conditional herd immunity, however, was attained while maintaining moderate mitigation measures (social distancing, school closed, mask-wearing and other self-care behaviors). None of the countries analyzed have returned to the pre-pandemic levels of activity and it is unclear if current population immunity will halt the viral spread after

removal of all mitigation measures. Furthermore, long-term herd immunity could be also challenged by waning immunity and dissemination of more infectious SARS-CoV-2 variants [39]. Both factors seems to have shaped the third epidemic wave in Israel [40, 41, 42, 43] Our study supports that after a transient period of decoupling in Israel, population mobility and viral transmissions were coupled again as Delta variant spread in both unvaccinated and fully-vaccinated individuals.

The same phenomena, however, was not observed in South America after introduction of Delta. Despite Delta progressively replaced the other SARS-CoV-2 variants between July and November 2021, the total number of SARS-CoV-2 cases in South America remained relatively constant, supporting a regional conditional herd immunity against Delta [1]. Several factors may explained such observation. First, herd immunity through natural infection seems to be less susceptible to waning immunity than by vaccination [44, 45, 46] and South American countries with a high natural immunity wall might be better prepared to limit the expansion of Delta variant than those with a large vaccine immunity wall. Second, hybrid immunity (natural infection plus vaccination) might provide longer lasting and stronger protection against infection than vaccine-induced immunity [47] and a high proportion of partial or fully vaccinated individuals in South America may be in that condition. Third, some South American countries like Chile and Uruguay started the administration of a vaccine booster around early August 2021, soon after first detection of Delta variant.

Our study has some important limitations: (i) difficulty to estimate precisely the IFR and consequently to have a precise estimate of the cumulative number of naturally infected people at decoupling point in each country; (ii) sub-reporting of SARS-CoV-2 deaths might underestimate the cumulative number of infections and thus the cHIT; (iii) the assumption that partially vaccinated people did not greatly contribute to reduce viral transmissions might have also underestimate the number of vaccine-immune individuals and the actual cHIT; (iv) on the other hand, although we assumed some overlap between vaccinal immunity and natural immunity, the precise fraction of fully vaccinated individuals that were previously infected is unknown. Because of these limitations, the precise cHIT estimated here should be interpreted with caution and should not be considered as general reference values for other countries.

In summary, our study supports that populations from the South American Southern cone probably achieved the cHIT to contain the further spread of SARS-CoV-2 variants Gamma and Lambda at around mid-2021. Presumed herd immunity was probably mostly attained by natural infection in Argentina, Brazil and Paraguay, and by a mixture of natural infections and vaccination in Chile and Uruguay. The widespread used of the Coronavac inactive viral vaccine in South America was not only effective to prevent the severe forms of COVID-19 disease but also has the potential to contain the community spread of highly transmissible SARS-CoV-2 regional variants. Inactivated SARS-CoV-2 vaccines, combined with other vaccines and mitigation measures, may thus represent a relevant tool to control the COVID-19 pandemic especially under the severe limitation of vaccine supplies faced by many countries around the world. Our findings stress that the conditional herd immunity status might be rapidly lost if vaccine-induce neutralizing antibodies decrease over time and/or immune escape SARS-CoV-2 variants are either introduced from abroad or evolved locally.

4 Methods

4.1 Data and code availability

The SARS-CoV-2 incidence data, viral effective reproduction number R_t (also indicated as reproduction rate), confirmed deaths, vaccinated people, and other epidemiological indicators were retrieved from Our World in Data (OWID) [1]. Mobility index was estimated from the six indicators categories (retail and recreation, grocery and pharmacy, parks, transit stations, workplaces, and residential) provided by Google COVID-19 Community Mobility Reports [48]. For the sake of reproducible research, the code used to obtain all the results and figures is available at `https://github.com/marfiori/covid19-decoupling`.

4.2 Estimation of the viral effective reproduction number and decoupling time

As the correlations between the six different possible regressors are large, we construct indices that are more robust along time and different countries, to avoid overfitting. In order to do this, we choose for each country the three categories that give the best fit among all possible combinations. Although the categories may vary, the obtained fit quality is relatively robust over different time intervals. The six mobility time series were smoothed by averaging over a 14 days sliding window.

For each country, we selected a time period consisting of 75 days before the start of the vaccination campaign, and 55 days after, ending up with a 130-days period to carry out the estimation. Given a set of three mobility categories, we fitted a linear regression model to the viral effective reproduction number R_t, lagged a certain time period. This time shift was chosen as the lag that maximizes the correlation of the regression. This procedure was repeated for each combination of three categories among the six mobility measures provided by Google, and the combination achieving the best regression result was kept. It should be noted that, since the six categories are highly correlated, other combinations of three categories achieve similar fitting results, and therefore the chosen categories are not necessarily informative by themselves.

Using the coefficients obtained in this 130-days period, and rest of the mobility time series, we computed the predicted viral reproduction number $\hat{R}_t$. The procedure was tested using periods of different lengths for the estimation, and the results in the cHIT are robust along the different experiments.

When population mobility and viral transmission are coupled, the coupling ratio $\hat{R}_t/R_t$ oscillates around one (0.90-1.10). Departing from a certain moment, the $\hat{R}_t$ becomes much higher than the R_t, revealing the decoupling between population mobility and viral spread resulted. We defined the **decoupling time** D_t as the moment when the coupling ratio $\hat{R}_t/R_t$ definitely exceeds the value 1.10, i.e. the last crossing over 1.10.

4.3 Estimation of the IFR and immune population

As it is well known, the estimation of the infection fatality rate has been a hard task during all the pandemic. The cryptic circulation of the virus (due to asymptomatic infections) and different variants made that in fact this quantity varies along time and populations. Here we took into account the most relevant variable to compute it, that is the age structure of the population. We then took IFR by age taken from [49] and adjusted to the population pyramid of each of the considered countries [50]. Confidence intervals were calculated by considering the (very large) confidence intervals available from [49] and estimating the interval for the whole population as the weighted average of the positions for the maximum or minimum of the age-classes intervals. Only one exception was introduced: in the Uruguayan case, the confidence interval can be reduced because the IFR must be smaller than the Case Fatality Rate (CFR). Imposing this constraint the maximum possible value in the Uruguayan case is reduced (we obtained the CFR corresponding to July 31 from [1]) the other countries being unaffected. This IFR estimation was confirmed using an alternative methodology for the case of Uruguay, following [51], which led to similar results, but with slightly larger confidence intervals.

The percentage of immune population was computed considering the immunity achieved by vaccination (including its effectiveness), and natural infection. However, many people who gained immunity by natural infection, might have gotten vaccinated as well. In order to avoid the over estimation resulting from counting twice those subjects, we subtracted the intersection of these fractions, under the assumption that they are independent. Observe that this assumptions gives us a lower bound on the estimation of immune population.

For a given country, let us denote by FV the proportion of fully vaccinated people, by NI the proportion of people with immunity by natural infection, and by VE the vaccine effectiveness of the country, computed by combining the effectiveness of each vaccine type (VIN, ADV, RNA) using the proportion of vaccines used in the country (see Table 1). We assumed a perfect immunization due to natural infection. That is, we neglected in the present analysis the number of re-infections. Furthermore, let us denote by IM the estimation of the proportion of immunized population. Then, the computation described above is as follows:

$$IM = (FV - FV \times NI) \times VE + NI.$$

Here the product $FV \cdot NI$ accounts for the intersection of the populations, which is subtracted from the vaccinated population before the effectiveness factor is applied. As described through the text, the proportion

of people with immunity by natural infection is inferred from the confirmed deaths, using the estimated IFR.

Observe that due to the vaccine effectiveness, the percentage of fully vaccinated people may by greater than the percentage of immunized population.

Additional Information

Author contributions

MF carried out the numerical experiments, wrote the code and prepared the figures. GB wrote the main manuscript text, and provided insight in the biological processes. NW contributed with ideas in the experiments, and computed the IFR taking into account the age distribution for each country. FL contributed to the processing of the mobility data. AF contributed to the code, and provided independent computations which corroborate the numerical results. EM wrote the main manuscript text, and provided insight in the statistical analysis.

All authors conceived and design the study, contribute to data analysis, and review the final manuscript.

Competing interests

The authors declare no competing interests.

Acknowledgements

We are indebted to P. Bermolen, M. Cerminara, M. I. Fariello, F. Paganini, R. Radi, M. Reiris, A. Rojas de Arias and C. E. Schaerer, for useful discussion and support. Any errors are the responsibility of the authors.

References

[1] Ritchie H. et al. Coronavirus Pandemic (COVID-19), (2020). Published online at OurWorldInData.org. Retrieved from: https://ourworldindata.org/coronavirus. Accessed 2021-08-28.

[2] Torres C. et al. Surveillance of SARS-CoV-2 variants in Argentina: detection of Alpha, Gamma, Lambda, Epsilon and Zeta in locally transmitted and imported cases. medRxiv 2021.07.19.21260779. https://doi.org/10.1101/2021.07.19.21260779

[3] Rego N. et al. Real-Time Genomic Surveillance for SARS-CoV-2 Variants of Concern, Uruguay. *Emerg. Infect. Dis.* **27**, 11 (2021).

[4] Ministério de Saúde. Fundaçao Oswaldo Cruz. Frequencia das pricipais linhagens do SARS-CoV-2 por mês de amostragem. Accessed 2021-09-02.

[5] Ministerio de Salud, Chile. Informe epidemiológico. Vigilancia genómica de Sars-cov-2 (COVID-19) Chile 08 de agosto de 2021. Accessed 2021-09-02.

[6] Boumans, M. Flattening the curve is flattening the complexity of covid-19. *HPLS* **43**, 18 (2021).

[7] Kraemer, Moritz U. G. et al. The effect of human mobility and control measures on the COVID-19 epidemic in China. *Science* **368**, 493–497 (2020).

[8] Hamada S. Badr et al. Association between mobility patterns and COVID-19 transmission in the USA: a mathematical modelling study. *Lancet Infect. Dis.* **20**, 1247–54 (2020).

[9] Leung, K., Wu, J.T. and Leung, G.M. Real-time tracking and prediction of COVID-19 infection using digital proxies of population mobility and mixing. *Nat. Commun.* **12**, 1501 (2021).

[10] Sulyok, M., and Walker, M. Community movement and COVID-19: A global study using Google's Community Mobility Reports. *Epidemiology and Infection,* **148**, E284 (2020).

[11] Athanasios A., Irini F., Tasioulis T., Konstantinos, K. Prediction of the effective reproduction number of COVID-19 in Greece. A machine learning approach using Google mobility data. medRxiv 2021.05.14.21257209; https://doi.org/10.1101/2021.05.14.21257209

[12] Nouvellet, P., Bhatia, S., Cori, A. et al. Reduction in mobility and COVID-19 transmission. *Nat. Commun.* **12**, 1090 (2021).

[13] Unwin, H.J.T., Mishra, S., Bradley, V.C. et al. State-level tracking of COVID-19 in the United States. *Nat. Commun.* **11**, 6189 (2020).

[14] Milman, O., Yelin, I., Aharony, N. et al. Community-level evidence for SARS-CoV-2 vaccine protection of unvaccinated individuals. *Nat Med* **27**, 1367–1369 (2021).

[15] Pritchard, E., Matthews, P.C., Stoesser, N. et al. Impact of vaccination on new SARS-CoV-2 infections in the United Kingdom. *Nat. Med.* **27**, 1370–1378 (2021).

[16] Google Mobility Reports. See how your community is moving around differently due to COVID-19. Accessed July 29, 2021.

[17] Jara, A. et al. Effectiveness of an Inactivated SARS-CoV-2 Vaccine in Chile. *New England Journal of Medicine,* **385**, 875–884, (2021).

[18] Cerqueira-Silva T. et al. Influence of age on the effectiveness and duration of protection in Vaxzevria and CoronaVac vaccines. medRxiv 2021.08.21.21261501. https://doi.org/10.1101/2021.08.21.21261501

[19] Sauré D. et al. Dynamic IgG seropositivity after rollout of CoronaVac and BNT162b2 COVID-19 vaccines in Chile: a sentinel surveillance study. *The Lancet, Infectious Diseases*,x¡ September 09, 2021. https://doi.org/10.1016/S1473-3099(21)00479-5

[20] Ministerio de Salud. Argentina. Datos Abiertos del Ministerio de Salud. Accessed 2021-08-27.

[21] Ministério de Saude. Brasil. Covid-19 Vacinaçao. Doses Aplicadas. Accessed 2021-08-26.

[22] Ministerio de Salud. Chile. Vacunación SARS-Cov-2. Accessed 2021-08-26.

[23] C. E. Schaerer. Personal communication, 2021-08-24.

[24] Ministerio de Salud Pública. Uruguay. Catálogo de datos abiertos. Accessed 2021-08-26.

[25] Rossman, H., Shilo, S., Meir, T. et al. COVID-19 dynamics after a national immunization program in Israel. *Nat. Med.* **27**, 1055–1061 (2021).

[26] Omer S. B., Yildirim I, Forman H. P. Herd Immunity and Implications for SARS-CoV-2 Control. *JAMA* **324**, 2095–2096 (2020). doi:10.1001/jama.2020.20892

[27] Marcus Carlsson, Cecilia Söderberg-Nauclér. Indications that Stockholm has reached herd immunity, given limited restrictions, against several variants of SARS-CoV-2 medRxiv 2021.07.07.21260167; https://doi.org/10.1101/2021.07.07.21260167

[28] M. Gabriela et al. Individual variation in susceptibility or exposure to SARS-CoV-2 lowers the herd immunity threshold medRxiv 2020.04.27.20081893. https://doi.org/10.1101/2020.04.27.20081893

[29] Tom Britton, Frank Ball, and Pieter Trapman. A mathematical model reveals the influence of population heterogeneity on herd immunity to SARS-CoV-2. *Science*, **369** 6505, 846–849 (2020).

[30] Infección por COVID 19: estudio seroepidemiológico de cohorte de base poblacional estratificado por edad en Asunción y Central. Sequera G. et al. http://dgvs.mspbs.gov.py/files/img/archivos/Estudio_seroepidemiologico.pdf Accessed 2021-09-01.

[31] Miraglia J.L., et al. A seroprevalence survey of anti-SARS-CoV-2 antibodies among individuals 18 years of age or older living in a vulnerable region of the city of São Paulo, Brazil. *PLoS ONE* **16**, (7): e0255412 (2021).

[32] Ministerio de Ciencia, Tecnología, Conocimiento, e Innovación de Chile. https://github.com/MinCiencia/Datos-COVID19/blob/master/output/producto83/vacunacion_fabricantes_1eraDosis.csv Accessed 07-23-2021.

[33] Al Kaabi N. et al. Effect of 2 Inactivated SARS-CoV-2 Vaccines on Symptomatic COVID-19 Infection in Adults: A Randomized Clinical Trial. *JAMA*, **326**, 35–45 (2021).

[34] Dagan, N. et al. BNT162b2 mRNA Covid-19 Vaccine in a Nationwide Mass Vaccination Setting. *New England Journal of Medicine*, **384**, 1412–1423 (2021).

[35] Stephen J. T., et. al. Six Month Safety and Efficacy of the BNT162b2 mRNA COVID-19 Vaccine. medRxiv 2021.07.28.21261159; https://doi.org/10.1101/2021.07.28.21261159

[36] Anderson, R. M., Vegvari, C., Truscott, J., Collyer, B. S., Challenges in creating herd immunity to SARS-CoV-2 infection by mass vaccination. *The Lancet* Comment volume **396** 1614–1616 (2020).

[37] Brüningk, S. C. et al. Determinants of SARS-CoV-2 transmission to guide vaccination strategy in an urban area. medRxiv 2020.12.15.20248130. https://doi.org/10.1101/2020.12.15.20248130

[38] Hjorleifsson, K. E. et al. Reconstruction of a large-scale outbreak of SARS-CoV-2 infection in Iceland informs vaccination strategies. medRxiv 2021.06.11.21258741.

[39] Aschwanden, C. Why herd immunity for covid is probably impossible. *Nature*, **591**, 520–522 (2021).

[40] Pouwels, K. B. et al. Impact of Delta on viral burden and vaccine effectiveness against new SARS-CoV-2 infections in the UK. medRxiv 2021.08.18.21262237. https://doi.org/10.1101/2021.08.18.21262237

[41] Goldberg Y. et al. Waning immunity of the BNT162b2 vaccine: A nationwide study from Israel. medRxiv 2021.08.24.21262423. https://doi.org/10.1101/2021.08.24.21262423

[42] Israel, A. et al. Elapsed time since BNT162b2 vaccine and risk of SARS-CoV-2 infection in a large cohort medRxiv 2021.08.03.21261496. https://doi.org/10.1101/2021.08.03.21261496

[43] Mizrahi B. et al. Correlation of SARS-CoV-2 Breakthrough Infections to Time-from-vaccine; Preliminary Study. medRxiv 2021.07.29.21261317. https://doi.org/10.1101/2021.07.29.21261317

[44] Gazit, S. et al. Comparing SARS-CoV-2 natural immunity to vaccine-induced immunity: reinfections versus breakthrough infections. medRxiv 2021.08.24.21262415; https://doi.org/10.1101/2021.08.24.21262415

[45] Wang, Z., Muecksch, F., et al. Naturally enhanced neutralizing breadth against SARS-CoV-2 one year after infection. *Nature*, **595**, 426–431 (2021).

[46] Cohen et al., 2021, *Cell Reports Medicine* **2**, 100354 (2021).

[47] Crotty, S., Hybrid immunity. *Science* **372**1392–1393, (2021).

[48] Aktay A. et al., Google COVID-19 Community Mobility Reports: Anonymization Process Description (version 1.1). November 4, (2020). arXiv:2004.04145v4 [cs.CR]

[49] Verity, R. et al., Estimates of the severity of coronavirus disease 2019: a model-based analysis. *The Lancet, Infectious Diseases*, **20**, 669–677 (2020).

[50] Population Pyramids of the World from 1950 to 2100. https://www.populationpyramid.net/. Accessed 2021-08-31.

[51] Moghadas, S. et al. Population Immunity Against COVID-19 in the United States. *Annals of Internal Medicine*, https://doi.org/10.7326/M21-2721

[52] Killick, R., Fearnhead, P., and Eckley, I. A. Optimal Detection of Changepoints With a Linear Computational Cost. *Journal of the American Statistical Association*, 107, 1590–1598 (2012).

[53] Cori, A., Ferguson, N., Fraser, C. and Cauchemez, S. A New Framework and Software to Estimate Time-Varying Reproduction Numbers During Epidemics. *American Journal of Epidemiology*, 178(9), 1505–1512 (2013).

[54] Du Z, Xu X, Wu Y, Wang L, Cowling BJ, Meyers LA. Serial Interval of COVID-19 among Publicly Reported Confirmed Cases. *Emergent Infectious Diseases*, 26(6), 1341-1343 (2020).

[55] Arroyo-Marioli, F., Bullano, F., Kucinskas, S. and Rondón-Moreno, C. Tracking R of COVID-19: A new real-time estimation using the Kalman filter. *PLOS ONE*, 16, 1–16 (2021).

[56] Shumway, R. H., and Stoffer, D. S. *Time series analysis and its applications: With R examples* Springer, New York (2006).

A Supplementary Material

A.1 Additional countries

In figures A.1 and A.2 we provide the same analysis shown in figures 1 and 2 respectively, for the case of Israel and Italy. It can be observed that the same phenomenon described in the main text takes place in these countries. Namely, a first period where the mobility successfully fits and predicts the reproductive number R_t, and after the effect of the vaccination starts to complement the immunity from natural infection, a period where the R_t decouples from the mobility.

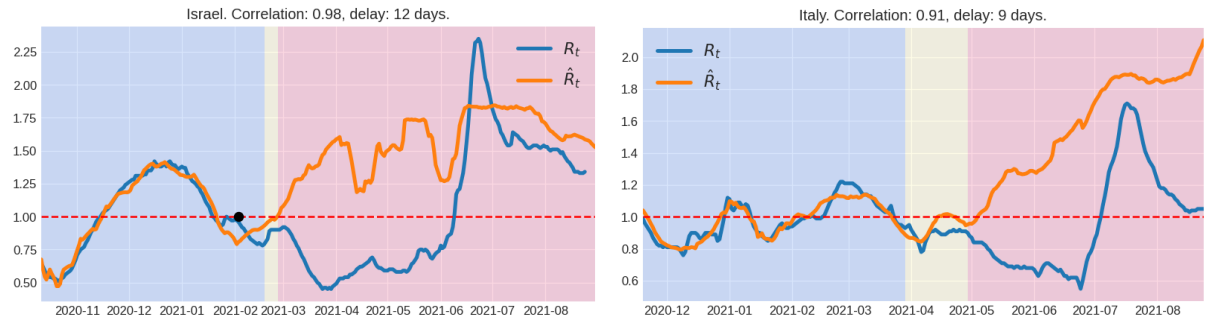

Figure A.1: Viral effective reproduction number R_t and its estimation $\hat{R}_t$ using mobility information. Background colors indicate the following time periods: in blue, the time period used to fit the linear model (see Section 4.2), in yellow, the period after the fitting, but before the decoupling point, and in red after the decoupling point. The black dot corresponds to the last time the reproductive number was above one. The correlation corresponds to the period used to fit the model. The delay indicated is the time-shift between the mobility time series and R_t in order to maximize the correlation in the linear regression.

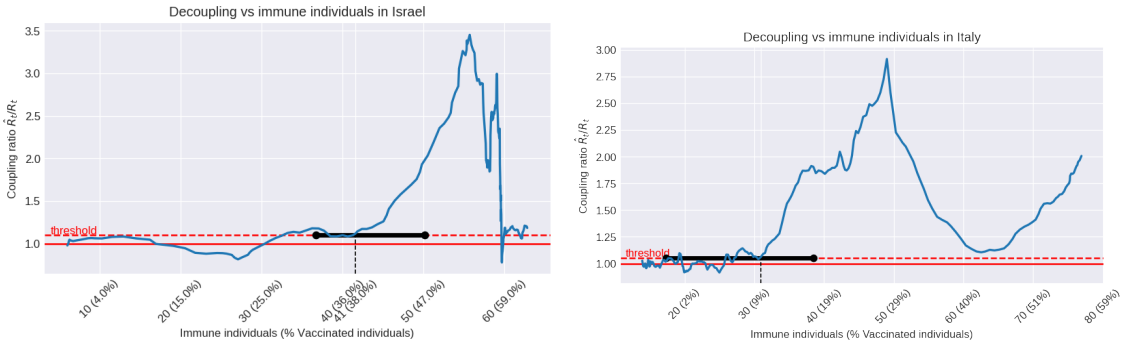

Figure A.2: Coupling ratio $\hat{R}_t/R_t$ plotted with respect to the percentage of immune population. During the first months of 2021 the coupling ratio varies around 1, which corresponds to the periods where the R_t and $\hat{R}_t$ are in concordance in Figure A.1. Immune population includes immunity achieved by vaccination (taking into account its effectiveness), and natural infection (see subsection 4.3). The percentage of people fully vaccinated is described as well.

A.2 Further methodological details and validation

A.2.1 Estimating the reproduction rate

For the analysis in this paper we considered several possible estimations of the time-varying reproduction rate R_t of the epidemic. We now briefly review the available approaches and explain our decision to settle on a given estimator for R_t.

A first approach, proposed in [53], consists on estimating R_t directly from incidence data I_t, the number of observed new cases. The estimation proceeds as follows: assume that when a person becomes infected, it can start spawning new infections from its contacts. These new infections will be reflected in the number of cases (become detected) after a *random* period of time, which can be modeled by a probability distribution w_s on $s > 0$. This is called the *serial interval* of the disease, and for SARS-CoV-2 it has been estimated by [54] as having a mean of 3.95 days and a standard deviation of 4.75 days. For definiteness we assume a discrete Gamma distribution for $\{w_s\}$ with these mean and variance.

Assuming that the number of contagions generated by an individual is Poisson and independent across individuals, the number of new infections at time t follows also a Poisson distribution given by:

$$I_t \sim \text{Poisson}\left(R_t \Lambda_t\right), \tag{1}$$

where R_t is the current reproduction rate that we wish to estimate, and Λ_t is given by:

$$\Lambda_t = \sum_{s>0} w_s I_{t-s}. \tag{2}$$

The intuition behind Λ_t is that this should be the average number of new infections reported at time t for a reproduction rate of 1.

The authors of [53] then propose to use a Bayesian approach. Assuming R_t is approximately constant over a window of length τ, and that a priori is distributed as a Gamma random variable with shape parameter a and scale parameter b, the a posteriori distribution of R_t can be computed and a suitable estimation of R_t is obtained as:

$$R_t = \frac{a + \sum_{k=t-\tau+1}^{t} I_k}{\frac{1}{b} + \sum_{k=t-\tau+1}^{t} \Lambda_k} \tag{3}$$

Eq. (3) has a simple intuitive explanation: besides a small bias from the a priori parameters, it is the ratio between the new observed cases in a given time window to the number of expected cases for a reproduction rate of 1.

The main advantage of this method is that it makes little assumptions on the dynamics of the epidemic, only dealing with disease specific parameters and the reasonable Poisson assumption on contacts. The main disadvantage is that, in order to be robust against the noise in observations and cope with weekly seasonal effects observed in the data, we have to employ a pretty large estimating window τ (typically between 7 and 14 days). This introduces a significant *lag* in the estimation. With data up to time t, we are estimating the value of R_t with a delay of up to 1 week. Since we are interested in the time correlations between mobility and the *current value* of the reproduction rate, this lag precludes us from using this robust estimator.

A second approach is proposed in [55], and is currently computed in real time for a list of countries in [1]. The authors assume a simple SIR model for the dynamics of currently active cases, which we denote by A_t to avoid using the standard name I since we reserve I for *incidence* or *new infections*.

The dynamics of the active cases follow the evolution equation:

$$A_t = A_{t-1} + \gamma\,(R_{t-1} - 1)\,A_t. \tag{4}$$

Here $1/\gamma$ is the recovery rate, i.e. the average time a person stops spreading the disease. In the typical SIR model, $R_t = \beta_t S_t(N)$, where β_t is the current level of social interaction and S_t/N the ratio of susceptible population. However, since we are interested in quantifying only the reproduction rate, we can employ directly eq. (4).

A simple transformation of (4) expresses the *growth rate* of the active cases as a function of R_t:

$$gr(A_t) := \frac{A_t - A_{t-1}}{A_{t-1}} = \gamma(R_{t-1} - 1). \tag{5}$$

Moreover, for small relative increments this can be further simplified using the approximation $\log(1+x) \approx x$ to write:

$$\nabla \log(A_t) = \gamma(R_{t-1} - 1), \tag{6}$$

where ∇ is the usual difference operator.

Since most of the data available is for *incidence* of new cases I_t, in order to construct the time series A_t one resorts again to the SIR model equations to write:

$$A_t = (1-\gamma)A_{t-1} + I_t. \tag{7}$$

The complete procedure is as follows: given a time series data from case counts I_t, construct the series of active cases using (7). Then model the growth rate evolution of A_t by using a simple *local level model* [56] for the trend in the reproduction rate R_t given by:

$$\nabla \log A_t = \gamma(R_{t-1} - 1) + \varepsilon_t, \tag{8a}$$

$$R_t = R_{t-1} + \eta_t. \tag{8b}$$

where ε_t, η_t are measurement noises assumed Gaussian. A suitable estimation of R_t can be directly obtained from eqs. (8) by applying the Kalman filtering technique [56]. The main advantages of this approach are two-fold: first they are extremely robust to noise in the measurements I_t and consequently A_t. The second advantage is that the estimate is real-time, i.e. it introduces no lag on the trend. This is perfectly suited for our purposes where we want to characterize the time correlation with the mobility estimation.

During preparation of this manuscript, we enhanced the model in eqs. (8) to include cyclic components in order to model systematic weekly trends in the data. However, inclusion of these trends did not change significantly the estimated trend of the R_t trajectory, so for all our analysis, we settled on the local level model approach and Kalman filtering of (8).

A.2.2 Backtesting/Validation of regression

Although the regression of the mobility features to the R_t is fitted in the period with blue background in Figure 1, and therefore period with yellow background serves as a validation of this regression up to the decoupling time, in this section we provide further details and validation.

For all five countries, we took the period prior to the decoupling time, and divided it into two sections of approximately the same length. The first period is used to fit the regression parameters, and the second period is used to validate the fitting. Additionally, we compute the variance of the regression parameters in the standard way, and use them to draw Monte Carlo trajectories in order to build error bands around the regression curves. The results are shown in Figure A.3, where the correlation in both the training and validation period are also reported. The results tend to reasonably validate the obtained the regression.

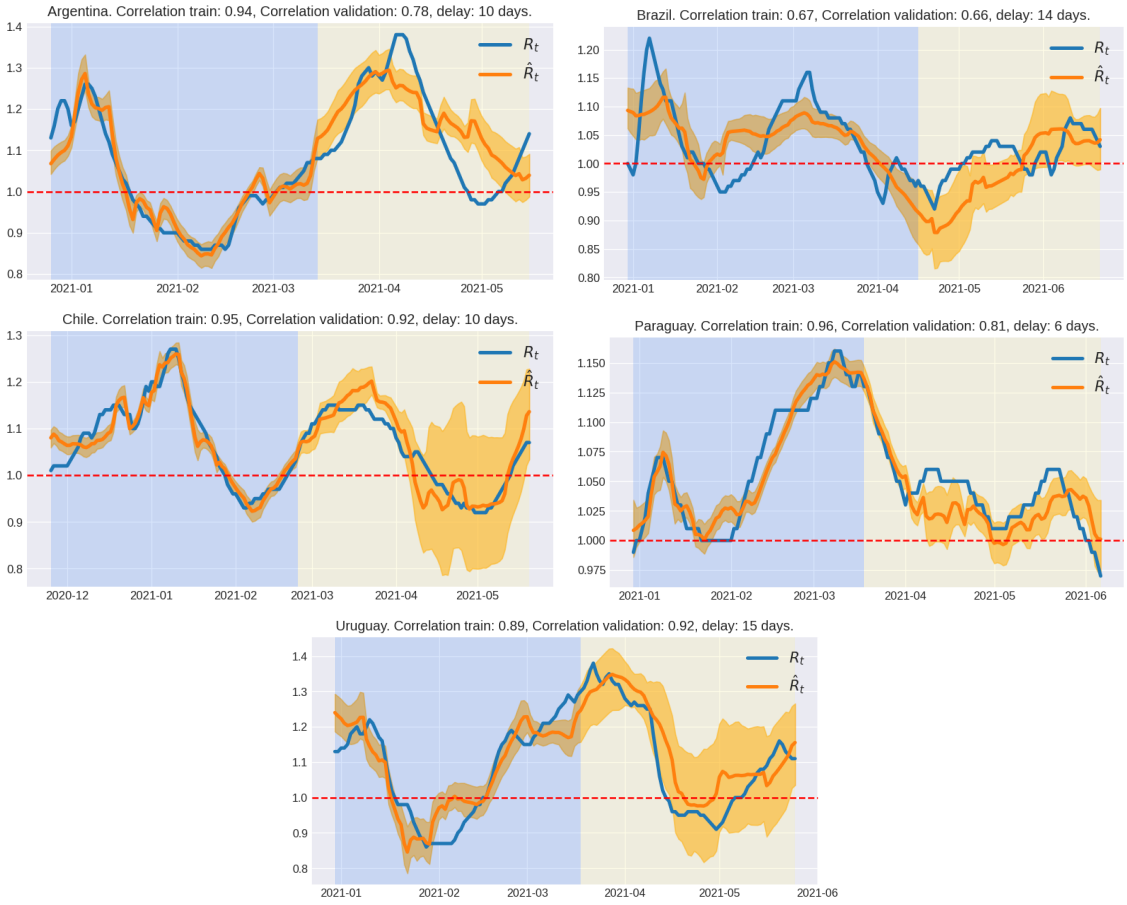

Figure A.3: Backtesting/validation of regression. The period with blue bakcgound is used to compute the regression, and the period with yellow background is used to validate the fitting. Error bands computed by Monte Carlo simulations, using the covariance of the regression parameters. The correlation in both the training an validation periods are reported in each panel.

A.2.3 Sensitivity to the threshold

As described in the main text, the decoupling time T_D was defined as the moment when the coupling ratio $\hat{R}_t/R_t$ definitely exceeds the threshold 1.10. In order to study the sensitivity to the value of this threshold, as well as to validate the methodology, we expose two additional experiments.

First, we present the decoupling time T_D and the corresponding immunity cHIT for several values of the threshold. It can be observed in Table 2 that the obtained cHIT values fall inside the confidence intervals in Table 1, and actually they are are very close to the central cHIT values presented.

Second, we present a decoupling time detection by means of an alternative method. Figure A.4 shows the coupling ratio $\hat{R}_t/R_t$, as well as the detected decoupling time D_t detected by the threshold (in dashed red),

Country	CPD	Threshold	T_D	cHIT
Argentina	May. 29	1.05	May. 30	29 %
		1.10	Jun. 02	29 %
		1.15	Jun. 03	30 %
		1.20	Jun. 06	33 %
Brazil	Jun. 22	1.05	Jun. 19	44 %
		1.10	Jun. 23	45 %
		1.15	Jun. 24	45 %
		1.20	Jun. 25	46 %
Chile	May. 28	1.05	May. 18	42 %
		1.10	May. 22	43 %
		1.15	May. 26	44 %
		1.20	May. 30	45 %
Paraguay	Jun. 12	1.05	Jun. 09	33 %
		1.10	Jun. 11	36 %
		1.15	Jun. 18	37 %
		1.20	Jun. 26	38 %
Uruguay	Jun. 10	1.05	May. 27	33 %
		1.10	May. 29	33 %
		1.15	Jun. 01	34 %
		1.20	Jun. 13	36 %

Table 2: Decoupling time (T_D) and cHIT (conditional herd immunity threshold) for different threshold values. The decoupling time detected by the Change Point Detection method (CPD) is also reported for comparison.

and the result of a standard Change Point Detection (CPD) algorithm [52] (in blue). It can be observed that both methods yield compatible results in all five countries.

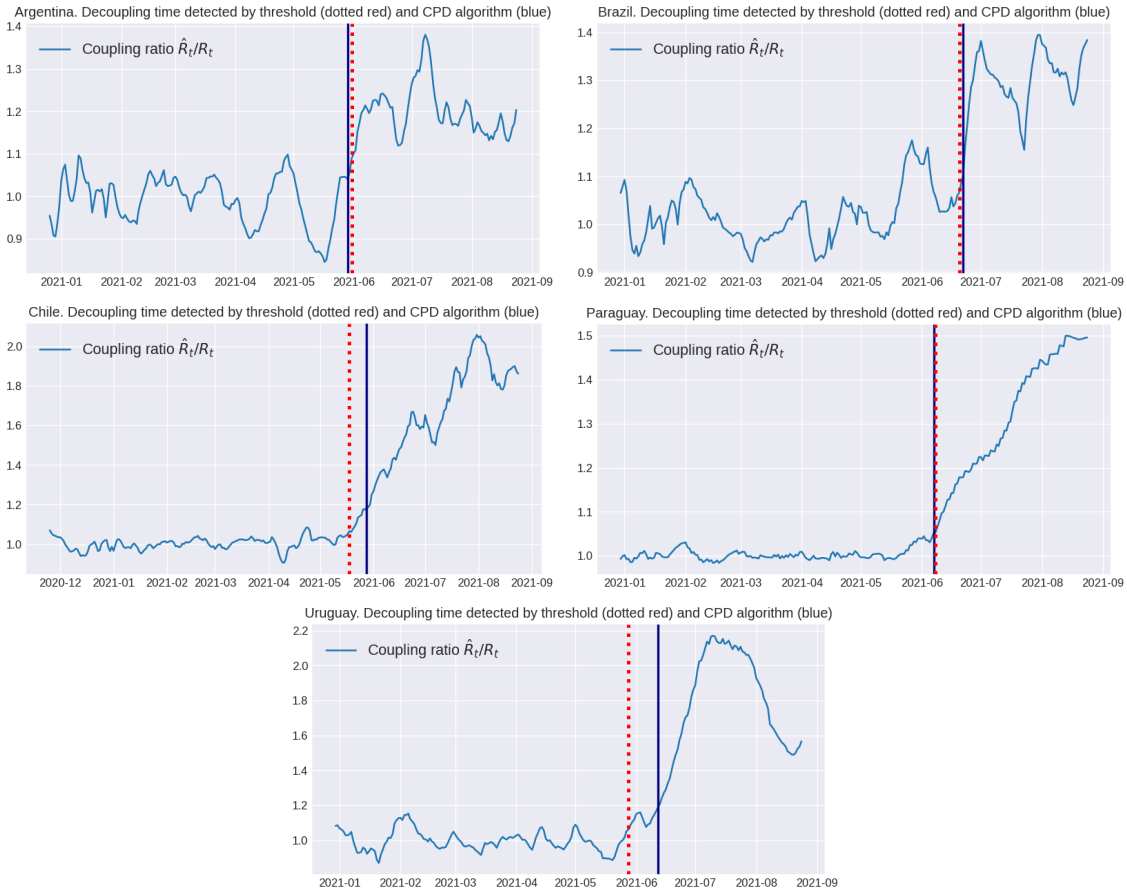

Figure A.4: Comparison of decoupling time detection as described in the main text (threshold), and by using a standard Change Point Detection method. Observe that the larger difference is only 12 days.